An Artificial Neural Fuzzy Inference System Based on a Grey Wolf Optimized Convolution Neural Network for Efficient Cardiovascular Disease Prediction

Arockia Raj Y[1]*, Uthama kumar A[2], S Pournima[3], V.Krishna Meera[4]

[1]Assistant Professor, Department of Computer Science and Engineering, PSNA college of Engineering and Technology, Dindigul 624 622, Tamil Nadu , India .Email: y.arockiaraj@psnacet.edu.in*

[2]Associate Professor, Department of MCA, AMC Management College, Bannerghatta Road, Bengaluru India 560083.Email: uthama.kumar@amceducation.in

[3]Assistant Professor, Department of CSE, Sona College of Technology (Autonomous), Salem 636 005. Tamil Nadu, India. Email: pournimascse@gmail.com

[4]Assistant Professor, Department of Electronics and Communication Engineering, Ramco Institute of Technology, Rajapalayam-626117, Virudhunagar, Tamil Nadu, India. Email: krishnameera@ritrjpm.ac.in

Abstract: Increasing variations in daily human lifestyle, such as food habits, work routines, and modern communication methods, have significantly influenced human health. Cardiovascular diseases (CVDs) remain among the most prevalent and life-threatening conditions, often leading to sudden cardiac arrest, and other chronic diseases. The advancement of big data and Artificial Intelligence (AI) has revolutionized disease detection, yet challenges persist due to the complex nature of disease properties and unknown feature dependencies. To resolve these problems, an ANFIS-based CVD disease prediction system using a Grey Wolf Optimized Convolutional Neural Network (GWO-CNN) is proposed in the paper. Heart Rate Variability (HRV) is utilized to estimate disease impact rates, followed by Structural Cascaded Pattern Mining (SCPM) to construct disease patterns based on high-impact margins. Feature selection is conducted using the ANFIS model, which effectively reduces irrelevant features, and the classification is performed using GWO-CNN to identify CVD risk levels. The experimental results section evaluates the model's performance through accuracy, precision, recall, specificity, and F1-score, demonstrating superior results compared to conventional methods. The FGWO-CNN model, which integrates GWO with a Deep CNN (DCNN), achieved superior performance compared to baseline models such as Random Forest with an Improved Linear Model (RERF-ILM) and Queen McCluskey Binary Classifier (QMBC). The proposed system achieves high performance, improving prediction accuracy up to 96% while maintaining a low false positive rate and reduced time complexity. This approach enhances early CVD detection, enabling timely interventions and improving health outcomes through performance measurement.

Keywords: : cardiovascular disease (CVD), Artificial Neural Fuzzy Inference System (ANFIS), Grey Wolf Optimized Convolutional Neural Network (GWO-CNN), Heart Rate Variability (HRV), Structural Cascaded Pattern Mining (SCPM), Feature Selection, Machine Learning (ML), Deep Learning (DL)..

Introduction

The Heart disease (HD) is a disease that affects more than 64 million people worldwide, and its incidence and prevalence continue to rise. Patients with HD often suffer from reduced quality of life and early death. Under these circumstances, international guidelines strongly recommend interventions to prevent the progression of HD. Early diagnosis of these diseases is essential so that preventive measures can be taken to avoid severe cases [Zhou, C et al, (1)]. Most cardiovascular prognostic studies have used advanced technologies such as artificial intelligence (AI) and deep learning in the last decade.

Hence, timely treatment and early identification of CVD can greatly alleviate symptoms and enhance cardiac function. This approach will bolster healthcare systems by enabling early intervention and customized treatment plans. Prognostic insights regarding CVD can help avert the need for surgical procedures, thereby lowering surgical expenses [Naser, M. A (2)]. Early identification of heart disease can lessen the overall toll of mortality associated with it. CVD is not limited to heart-related complications alone; it can also be triggered by physiological and psychological factors such as shortness of breath, heartburn, right shoulder pain, and backache. The complexity of symptoms often leads to misdiagnosis, causing delays in treatment and increasing mortality rates [A. M. Qadri et al (3)]. Existing diagnostic techniques face limitations in early-stage detection and accurate disease prediction, prompting researchers to explore more efficient and intelligent methods to enhance CVD diagnosis and risk assessment [A. A. Almazroi et al (4)]. The Cleveland Heart Disease Database at the University of California, Irvine (UCI) repository is the most widely used dataset for this type of research. It maintains records of patients associated with a specific hospital medical background. In the era of ML method, data analytics and medicine will converge to facilitate accurate disease diagnosis [Ram Kumar, R. P et al, (5)].

Machine Learning (ML) techniques have been extensively employed for the detection of CVD, leveraging algorithms such as Support Vector Machines (SVM), Logistic Regression (LR), Artificial Neural Networks (ANN), K-Nearest Neighbors (KNN), Naïve Bayes (NB), and Decision Trees (DT). These methods have demonstrated the potential to improve diagnostic accuracy by analyzing clinical data and identifying disease patterns [X. Yuan et al, (6)]. However, traditional ML-based models encounter several challenges, including non-mutual dependencies of features, increased feature dimensions, low precision, poor recall rates, and high false positive rates. Additionally, feature dependencies in ML models are highly sensitive to scaling, leading to inaccuracies in predictions. Accessing hospital databases on CVD data significantly aids early detection and diagnosis, improving disease outcomes [Baghdadi, N. A et al, (7)]. To overcome these limitations, Deep Learning (DL) approaches have been introduced to enhance diagnostic accuracy, optimize computational efficiency, and reduce the cost of disease prediction.

DL-based methodologies offer improved performance by leveraging advanced feature extraction techniques, such as convolutional and recurrent neural networks, for analyzing large-scale medical datasets. These methods provide better generalization and robust decision-making capabilities, which are crucial in medical diagnostics [G. N. Ahmad et al (8)]. Early death can be prevented by identifying those most vulnerable to heart disease and ensuring that they are treated appropriately. The ability to quickly, efficiently, and accurately diagnose heart disease is critical to taking preventive measures to avoid further complications and death [Manikandan, G. et al, (9)]. Providing cost-effective, high-quality healthcare is a significant challenge facing healthcare institutions. The patient's problem should be properly diagnosed and treated effectively to receive quality treatment. This research proposes an optimized deep learning model for CVD detection based on an Intelligent Big Data Analytics Model [G. N. Ahmad et al, (10)].

The paper contributes to CVD detection using the Intelligent Big Data Analytics Model and an optimized deep learning model. A combined feature selection and classification method based on an artificial neural fuzzy inference system is developed using GWO-CNN to improve performance accuracy. Furthermore, early heart disease detection can be provided using the ANFIS and GWO-CNN method based on the optimized DL model to be validated on UCI and other real-world datasets. In addition, it provides a framework that integrates intelligent feature selection that reduces redundant features with a DL model for advanced heart disease detection. Afterward, the reliability of optimal feature selection-based CVD detection is improved. Experimental results, evaluating accuracy, precision, recall, specificity, and F1-score, demonstrate the model's superior performance compared to conventional methods.

Literature Review

This The study Gayathri, R, et al [11] introduced a new method to enhance cardiac disease prediction accuracy using data augmentation and reinforcement learning. Combining these methods efficiently provides a powerful solution to the problems posed by complex cardiac data. Joshi et al, [12]

Classic techniques like linear regression and several ML methods, including SVM, have been established for the classification of heart disease. CVD remains one of the least understood yet critical health concerns, significantly impacting the human heart. Several studies have explored the application of ML techniques for early detection, risk assessment, and prediction of CVD.

S. E. A. Ashri et al. [13] proposed an approach that leverages data collection, preprocessing, and transformation techniques to enhance the accuracy of training models. Their work introduced hybrid classifiers combined with majority voting techniques to improve prediction accuracy. Additionally, they suggested a genetic algorithm-based feature selection method to optimize preprocessing, leading to enhanced prediction performance and reduced computational time. A. Rahim et al [14] developed an ML-based cardiovascular diagnosis framework, MaLCaDD, designed to predict CVD with high accuracy. The framework was specifically tailored to address challenges associated with missing values and data imbalance. Similarly, D. Cenitta et al. [15] explored advanced feature selection techniques that minimize the number of features while maintaining predictive performance.

Table 1. Machine Learning Technique based on CVD Prediction using Various Approaches and Datasets

Author	Year	Method	Dataset	Drawback
Saikumar, K [16]	2024	Gaussian Navies Bayes, Decision Tree (DT)	Radiology Dataset	CVD is a serious health problem affecting people in low- and middle-income countries.
Ogunpola [17]	2024	SVM, LR	Cleveland Clinic Foundation dataset	More research is needed to improve predictive models and detection.
Ramesh, B [18]	2024	Optimal Scrutiny Boosted Graph Convolutional Long Short-Term Memory (O-SBGC-LSTM)	Cleveland dataset	Since it affects multiple organs, early detection and treatment are essential to avoid long-term diabetes complications.
Trigka [19]	2025	Recurrent Neural Network (RNN)	CVD dataset	It often fails to analyze the complex interplay of multiple factors and the subtle patterns of increased risk.
Khan [20]	2024	LeNet and Gated Recurrent Unit (GRU)	Heart Disease Health Indicators Dataset	Accurate diagnosis of heart disease is vital in protecting patients from further harm.

As shown in Table 1, the proposed approaches based on machine learning techniques in the previous set can be evaluated using the dataset, and their shortcomings can be predicted.

Kapila et al. [21] introduced the Ensemble Queen McCluskey Binary Classifier (QMBC), which employs a multi-layer perceptron to improve CVD diagnosis. Abdellatif et al. [22] addressed the challenge of imbalanced datasets in heart disease detection by implementing the Synthetic Minority Over-sampling Technique (SMOTE). They demonstrated how feature models could be applied to standard datasets to enhance prediction performance. Additionally, data analysis methodologies such as the Korean National Health Insurance Service National Health Sample Cohort (KNHSC) have been employed to refine CVD risk prediction models. Ahmed et al, [23] conducts a comprehensive study of ensemble learning

and other hybrid ML techniques for predicting heart disease and improving diagnostic capabilities by using ensemble learning models to identify predictive patterns associated with heart disease. Siddiqui et al. [24] explored the use of heart rate variability (HRV) in predicting vascular events in hypertensive patients through an ML approach. Ullah et al, [25], propose a novel additive tree and random forest classifier trained on selected features, which achieves significant accuracy. Also, a comparison of the proposed method with state-of-the-art techniques on small and large datasets is presented.

Ishaq et al. [26] focused on analyzing heart failure survivor data, identifying critical predictive features using data mining techniques and random forests (RF). As stated, Venkatesh, C, et al [27] Integrating the two methods is anticipated to enhance the effectiveness of conventional techniques in forecasting CVD from clinical data. Additionally [27], DL methods can potentially lower mortality rates by predicting heart disease through clinical data and patient severity assessments.

Naeem et al. [28] tests were performed using the evaluation scale, and the results demonstrated that the model's accuracy was greater than 85% in most cases. Xiao et al. [29] developed lightweight CNN-based models for CHD diagnosis, addressing a key challenge in DL frameworks by selecting essential features for CNN training. Finally, Rehman et al. [30] the results show that the proposed Particle Swarm Optimization Artificial Neural Network (PSO-ANN) model achieved a higher accuracy of up to 93% in predicting CHD, compared to the 95.8% accuracy of traditional classifiers.

The Liao et al., [31] proposed a smart electronic health system leveraging IoT and ML to enhance healthcare delivery through predictive analytics. By integrating ANN, specifically a multilayer perceptron with a genetic algorithm and error-back propagation, the system improves cardiac disease prediction accuracy. The proposed Mu-LTM-based model achieved high performance with a coverage error of 97.94%, accuracy of 97.89%, sensitivity of 97.96%, and specificity of 97.99%. IoT sensors collect real-time patient data, which is stored in the cloud for analysis, ensuring efficient and proactive healthcare management. This approach outperforms existing models in predictive accuracy and precision, making it a signifi--
----

894905cant advancement in medical diagnostics.

The Molamasoumi et al., [32] proposed a hybrid ANFIS-GWO method, integrating the Adaptive Neuro-Fuzzy Inference System (ANFIS) with Grey Wolf Optimization (GWO) for liver disorder diagnosis. ANFIS leverages neural networks and fuzzy logic, while GWO optimizes its hyper-parameters to enhance model performance. Using a dataset of 7 attributes and 354 samples, the ANFIS-GWO method improves classification accuracy, sensitivity, and specificity. Experimental results show superior diagnostic performance compared to traditional Fuzzy Inference Systems (FIS) and non-optimized ANFIS models. This suggests that GWO significantly enhances the predictive capability of ANFIS in liver disease diagnosis.

Despite the advancements in ML techniques for CVD prediction, several critical research gaps

remain unaddressed. Many existing models lack scalability and real-world validation, as they are predominantly tested on small-scale or benchmark datasets rather than diverse, large-population datasets that better reflect real-world clinical settings. Moreover, while deep learning models such as convolutional neural networks (CNNs) and ensemble classifiers demonstrate high accuracy, their excessive computational costs and hardware dependencies limit their feasibility for real-time healthcare applications. Another significant limitation is the inadequate handling of real-time and streaming data, as most frameworks primarily focus on static datasets rather than continuous patient monitoring, which is essential for early intervention. Additionally, while feature selection techniques, including genetic algorithms and optimization-based approaches, enhance model performance, they often lack interpretability, making their integration into clinical decision-making challenging. Security and privacy remain major concerns in IoT-enabled and cloud-based healthcare models, as existing solutions provide only limited measures to mitigate potential data breaches and cyber threats. Furthermore, most studies fail to explore the integration of multi-modal health data, such as genetic information, ECG readings, and wearable sensor data, which could significantly improve predictive accuracy and reliability. Addressing these gaps will be crucial in developing more robust, efficient, and clinically applicable ML models for CVD prediction. To overcome these challenges, the proposed methodologies have been designed to enhance model scalability, optimize computational efficiency, facilitate real-time data processing, improve interpretability, strengthen security measures, and integrate multi-modal health data for comprehensive and accurate CVD prediction.

2.1 Limitations of the research works

Training on large datasets for improved validation accuracy is challenging.

However, the increasing complexity of clinical datasets makes it challenging to detect associations and makes accurate predictions difficult.

Given the numerous variables, professionals often find it challenging to assess each patient while considering this information.

A suitable and accurate automated computer-based decision support system is needed to reduce the cost of clinical problems.

Recognizing and treating this disease remains challenging due to inadequate physician skills, high treatment costs, and limited diagnostic tools affecting treatment options.

Proposed Methodology

The integration of big data analytics in healthcare has become essential for improving disease prediction, particularly in diagnosing CVDs. One of the major challenges in developing accurate prediction models is handling high-dimensional data, as excessive or irrelevant features can distort results. To address this issue, this paper proposes an Intelligent Big Data Analytics Model that leverages a hybrid approach, combining an ANFIS and a GWO-CNN to enhance CVD prediction. The ANFIS module is utilized for feature selection, effectively filtering out unrelated features to ensure the reliability of the dataset used for prediction. Additionally, HRV is analyzed to assess a patient's defect rate, enabling a comparison between actual and optimal margins to determine the severity of the illness. Furthermore, SCPM is employed to identify critical disease patterns and high-impact margins, ensuring accurate disease resemblance detection.

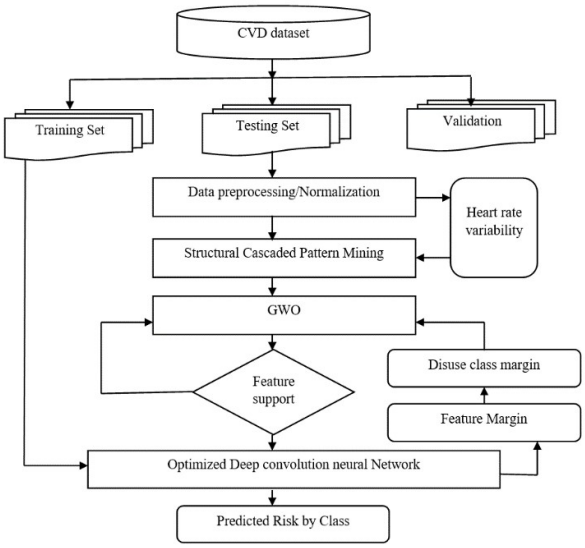

Fig. 1. Overview of Proposed Architecture Diagram

For classification, a GWO-CNN-based model is introduced, which enhances existing evolutionary computing algorithms to improve prediction accuracy. Prior to classification, the dataset undergoes big data normalization, a crucial preprocessing step that eliminates noise and inconsistencies, making it easier to analyze. The deep CNN-based classification approach is then applied to assess the effectiveness of the feature selection process and the overall efficiency of the model. This comprehensive approach offers a robust solution for CVD prediction by addressing key challenges, including dimensionality reduction, optimal feature selection, and enhanced deep learning-based classification.

By leveraging optimized feature selection techniques and credible deep learning algorithms, this model significantly enhances the accuracy and reliability of CVD prediction, contributing to improved disease management and patient outcomes. The overall framework of the proposed model is illustrated in Figure 1. The input dataset is partitioned into three subsets: training (60%), testing (20%), and validation (20%). Before processing, data normalization techniques are applied to remove unwanted noise and standardize data for improved efficiency. The GWO-CNN model is then evaluated on the preprocessed dataset using an advanced feature selection algorithm, which aims to extract only the most relevant features while optimizing computational efficiency. A stopping condition is defined to determine when the optimal subset of features has been selected. Once finalized, the GWO-based classification algorithm DCNN is trained on this refined dataset, ensuring enhanced classification accuracy while reducing computational complexity.

3.1 Normalization

In Data normalization plays a crucial role in improving processing efficiency, especially when dealing with varied data types, missing values, and out-of-range entries. In this study, normalization is applied using two primary methods. First, symbolic data mapping is performed using the map function in Python's Scikit-learn library, converting categorical symbols into unique numeric values for consistency. Second, the dataset X is transformed using a logarithmic equation, as presented in Equation (1), ensuring that all data points remain within a suitable range for further analysis.

$$X_{normalized} = log(X_i + 1) \quad (1)$$

Second, the feature data values are converted into the range between [0-1] using the Equation

$$X_{normalized}\ (X_n) = \frac{X_i - min(X_i)}{MAx(X_i) - Min(X_i)} \quad (2)$$

Noisy data can continuously increase computational costs and reduce system performance. Hence, using the normalization process, the noisy data are replaced with unique values to improve the system performance. The normalized features and record sets returned in X_n.

3.2 Heart Rate Variability (HRV)

The HRV analysis identifies differences in features by comparing actual CVD margins with expected variability rates. It extracts feature variations from normalized limits based on disease-specific margins, allowing for an accurate assessment of the disparity between the real disease risk and ideal

thresholds. This process ensures that only the most critical features are retained for heart disease prediction by systematically eliminating less relevant attributes during model training. The model ranks features based on their relevance using accuracy as a key metric. It takes the required number of components as input and prioritizes variables accordingly. Additionally, it categorizes features based on their actual significance, assigning a value of 1 for truly relevant features and **0** for irrelevant ones, using standard and abnormal variability rates as the determining factors.

Algorithms:

Input: Normalized Dataset X_n

For all verify medial actual margin ($A_m \rightarrow X_n$)

$A_m = \{ Xn = 1,2, \ldots \ldots . n; x \in y\}\ at\ all\ N\ data's$

Check all $X \longrightarrow Am$ initiated margin

Create a class for X→ difference.X_n

Step 1- For each class, check the maximum variability rate

A_m= argmax $j(s_i + x), where x \in d - s_i$ (3)

$Create\ a\ class\ for\ Cli <- X$

$x_{k+1} = x_{k+x}$

$n = n + 1$ (4)

End for

Step 2- Create comparative intersection margin for all class

$E = \{e_{ij}/i, j \in N\}$ Cl, (5)

$e_{ij} = \begin{cases} 1, if\ d(i,j) \leq R_n \\ 0 \quad Otherwise \end{cases}$ (6)

Compete the

$f(x) \rightarrow R_t\big(Val(fx_1) \leftrightarrow Val(fx_2)\big)$ (7)

Step 3- For each subset size s_i, do

Step 4 - End

Step 5 – Calculate the variability rate $X \longrightarrow s_i$

Step 6 - Determine the class variability $X_n \rightarrow X_{v1,V2}$ (8)

Step7- Return X_n

For all Features from ditsiest $f(x)$, $s_i -$ important variable, $N -$several nodes, $E -$estimation of the data $x\ and\ y$, then $R -$ Ideal and Actual margin. The CVD importance feature Limits are CRP, ESR, Cholesterol rate, Hypertension scale, Block chicness, thallus, and Albumin are essential features. This evaluates the risk class of feature weight difference Value to another Value to construct the type that confirms the CVD variability from the average level.

3.3 Structural Cascaded Pattern Mining (SCPM)

Features are organized into patterns based on cascaded marginal values**,** referred to as mutual feature support values**.** This approach helps eliminate non-contributory features by categorizing them according to their respective classes. By analyzing the disease impact**,** relevant features are identified and structured into a pattern using random variable modeling**.** This process establishes a probability support rate**,** where support values are assigned based on various risk factors, as determined by disease margins.

Algorithm steps:

Input: selected feature data

Calculate the extract feature

Ho (X) for the values $\{x1, x2, \ldots, xn\}$ can be given as

Ho(X) = $\sum_{i=1}^{n} p(x) \log_2 p(x)$ (9)

Here, p(x) represents the probability of extract value.

The two discrete X and Y random variables are given as

H(X|Y) = - $\sum_{i=1}^{n} \sum_{j=1}^{n} p(x_i, y_i)\ log_2\ p(x)/p(x,y)$ (10)

Where p(x,y) are joint probability to find the features.

Finalize the data

End

The variable probability factor features are grouped into pattern classes, each representing the

mean probability of disease occurrence across different patterns. This process eliminates features that lack significant relationships with the class factors, ensuring that only relevant attributes contribute to disease prediction. By selecting the most effective support feature margin rate for each class, the model enhances the accuracy and reliability of disease prediction, maintaining a well-defined disease prediction margin.

3.4 Artificial Neural Fuzzy Interference System(ANFIS)

In this section, the prediction of heart disease is performed using a highly non-linear, complex, and dynamic computational process known as the Adaptive Neuro-Fuzzy Inference System (ANFIS). ANFIS is capable of self-training using input training data to generate an initial membership function, which is then fine-tuned through back propagation or hybrid learning algorithms to minimize errors. Due to its adaptability and efficiency, ANFIS is widely applied in various predictive models, where it utilizes an appropriate number of rules to achieve high accuracy. However, the computational complexity of ANFIS increases exponentially as the number of inputs grows, leading to a greater number of regulatory and adjustable parameters, making the process more resource-intensive. Additionally, the design of the performance rules in ANFIS is directly influenced by the number of input parameters and their associated changeable parameters, which define the overall model performance.

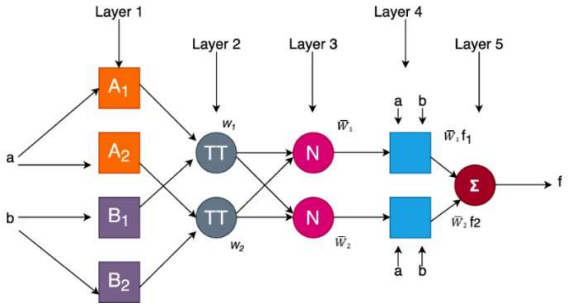

Fig. 2. ANFIS Working process

Figure 2 illustrates the ANFIS working process, depicting a basic ANFIS structure with two inputs and one output. In the context of cardiac analysis, this system generates four notification rules to aid in heart disease prediction.

As represented in Equations 11 and 12, each node within the fuzzification layer is treated as a square node, where specific parameters define the fuzzy membership grade. Here, E represents the output fuzzy membership grade, u denotes node, a *and* b are fuzzy input variables, while C *and* D represent fuzzy sets.

$$E_u^1 = \mu_{Cu}(a), \quad X!Y \qquad for\ u = 1,2 \qquad (11)$$

$$E_u^1 = \mu_{Du}(b), \qquad X!Y \quad for\ u = 3,4 \qquad (12)$$

As shown in Equation 12, each node can compute the membership of its input using a Gaussian membership function. Where z and σ −parameter sets, z-centre membership, position, σ- represents the membership function width.

$$E_u^1 = \mu_{Cu}(a) = f^{\frac{-1}{2}\left(\frac{a-z_u}{\sigma_u}\right)} \qquad (13)$$

The input can be processed, and the output evaluated for each node, as shown in Equation 14. Let's assume the Q-output of the layer.

$$E_u^2 = Q_u = \mu_{Cu}(a_1) \times \mu_{Du}(a_2) \times \mu_{zu}(a_3) \times \mu_{du}(a_4) \times \mu_{Fu}(a_5) \times \mu_{Eu}(a_6) \times \mu_{hu}(a_7) \quad u = 1,2, \ldots, \qquad (14)$$

As shown in equation 15, calculate the ratio of total rules of firing strength.

$$E_u^3 = \bar{Q} = \frac{Q_u}{Q_1 + Q'} \qquad u = 1,2,\ldots,7 \qquad (15)$$

Compute the adaptive layer node as shown in equation 16. Let's assume ($r_u + p_u + q_u + T_u$) −consequent parameters

$$E_u^4 = \bar{Q}_u g_u = \bar{Q}_u(r_u a_1 + p_u a_2 + q_u a_3 + C_u a_4 + D_u a_5 + z_u a_6 + d_u a_7 + T_u) \quad u = 1,2, \ldots,7 \qquad (16)$$

The total output is calculated as the sum of all input signals, as shown in Equation 17.

$$E_u^5 = b = \sum_u \bar{Q}_u g_u = \frac{\sum_u \bar{Q}_u g_u}{Q_u g_u} \qquad (17)$$

The basic rules for ANFIS calculations are assessed as shown in Equations 18 and 19. Let's assume

G_u and G_{u+1} as the optimized feature value, L_u, T_u, i_u, L_{u+1}, T_{i+1}, and i_{u+1} as the design parameters in the training process, G_u as the input node.

$$Rules_u = LG_u + T_u G_{u+1} + i_u \quad (18)$$

$$\mathrm{Rules_{u+1}} = \mathrm{L_{u+1}G_u} + \mathrm{T_{u+1}G_{u+1}} + \mathrm{i_{u+1}} \quad (19)$$

The fuzzy layer is used to determine the input values and their membership functions, as shown in Equation 20. Let's assume the μ_{gu}-membership function parameter.

$$K_{1,u} = \mu_{gu}(G_u) \quad (20)$$

Equation (21) represents the computation of the membership function using a Gaussian kernel. The membership function μ_{g_u} is mathematically expressed as:

$$\mu_{g_u} = exp\left(\frac{\|L_u - T_u\|^2}{2\, i_u^2}\right) \quad (21)$$

Where, L_u −represents a given data point or feature vector, T_u −target or reference point, i_u −parameter that controls the spread or variance of the Gaussian function. $\|L_u - T_u\|^2$ − squared Euclidean distance betweenL_u and T_u. The exponential function ensures that the membership value remains within the range [0,1], where closer values to T_u − higher membership scores.

Equation 22 shows the computation of the input signals that produce the layer's output, as expressed. Let's assume, $K_{2,u}$ −Output layer.

$$K_{2,u} = R_u = \mu_{g_u}(G_u) \times \mu_{g_u}(G_{u+1}) \quad (22)$$

Calculation of the firing strength normalization is shown in equation 23. Where $\bar{R}_u$signifies the normalization firing strength and u −node.

$$\mathrm{k_{3,u}} = \mathrm{\bar{R}_u} = \frac{\mathrm{R_u}}{\mathrm{R_1+R_2+R_3+R_4+R_5+R_6}}, \qquad \mathrm{u = 1,2,..,6} \quad (23)$$

The node functions are computed for the adaptive node in the layer as shown in Equation 24.

$$K_{4,u} = \bar{R}_u . Rules_u \quad (24)$$

Equation 25 shows that the total output is calculated from the summation of all input signals. Let's assume, $\sum_u R_u\, Rules_u$ − Label node.

$$\mathrm{K_{5,u}} = \sum_u \mathrm{R_u\ Rules_u} = \frac{\sum_u \mathrm{R_u Rules_u}}{\sum_u \mathrm{R_u}} \quad (25)$$

As described by the node functions in Equations 26 and 27, the ambiguity evaluates the adaptability of the nodes in the layer. Where, Y-adaptive node, m and n- denote inputs.

$$YG_{1,u} = \mu_{C_u}(m) \quad (26)$$

$$YG_{1,u} = \mu_{D_u}(n) \quad (27)$$

As shown in Equation 28, calculate the strength of the rules generated within the layer.

$$\mathrm{YG_{2,u}} = \mathrm{H_u} = \mu_{\mathrm{C_u}}(\mathrm{m}) * \mu_{\mathrm{D_u}}(\mathrm{n}) \quad (28)$$

Equations 29 and 30 show the normalized firing strength at this layer.

$$YG_{3,u} = \widehat{H}_u = \frac{H_u}{H_1+H_2}, \qquad u = 1,2 \quad (29)$$

The function of adaptive nodes is calculated as shown in equation 30. Let's assume H_u, Q_u, and p_u as Normalized values.

$$YG_{4,u} = \widehat{H}_u g_u = \widehat{H}_u(H_u m + Q_u n + p_u) \quad (30)$$

The final output can be calculated in this layer, as shown in Equation 31.

$$YG_5 = \sum_u \widehat{H}_u g_u = \frac{\sum_u H_u g_u}{\sum_u H_u} \quad (31)$$

In this category, the design of the efficiency rules used to determine the ANFIS allows for calculating the output layer depending on the number of input parameters selected for further classification units.

3.5 Grey Wolf Optimized Deep Convolutional Neural Network (GWO-DCNN)

A relevant subset of features can be selected based on the proposed feature selection algorithm using the normalized data as input to the feature selection stage. Furthermore, Pearson correlation-based PCRFS can perform feature selection methods of filter and wrapper methods. In addition, the evolutionary algorithm can exploit GWO through a subset of selected features to reduce the subset with essential factors. Optimization-based feature selection algorithms are more suitable and can improve classification accuracy with smaller feature sets than standard feature selection algorithms.

$$YG_5 \leftarrow xi, yi \quad (32)$$

Then, the Pearson correlation shows the relationship between data in the range [-1, 1]. Moreover, a positive 1 means positive correlation, 0 means no correlation, and negative means the data are described as negatively correlated. In contrast to other feature selection ML models, which remove

features at each stage, PCRFE eliminates irrelevant data at a similar period. This element of the hybrid approach makes it faster than filter, wrapper, and embedded file system approaches. The feature correlation coefficient is calculated using Equation (33).

$$PCorr_{xi,yi} = \frac{\sum_{i=1}^{n}(x_i-\bar{x})(y_i-\bar{y})}{\sqrt{\sum_{i=1}^{n}(x_i-\bar{x})^2}\sqrt{\sum_{i=1}^{n}(y_i-\bar{y})^2}} \quad (33)$$

Where xi, yi – features for correlation consideration. The value will reduce within the estimated interval [-1, 1]. A -1 or close to 1 designates a strong correlation between two features, and 0 shows a weak relationship between the two structures. Once the features have been combined, a threshold is used to rank the features. Low-ranking mechanisms are removed. The feature elimination procedure is shown in Equation (34).

$$\mathrm{PCRFE}(\mathrm{x_i}) = \sum_{\mathrm{i=1}}^{\mathrm{n}} \left(\mathrm{y_{i,j}} - \sum_{\mathrm{j=1}}^{\mathrm{d}} \mathrm{PCorr_{x_i,y_j}} \times \mathrm{x_i}\right)^2 \quad (34)$$

A subset of selected features can be optimized after removing irrelevant regions that do not fit the dataset using an optimization algorithm called GWO. Also, Gray Wolf is an advanced optimization technology based on wolf hunting behavior that can catch prey whenever they want. Target is organized and carefully maintained within populations [2]. GWO's hierarchy of leadership is divided into four levels: Alpha (α) - decision-making responsibility male or female; Beta (β) – helps alphas make decisions; Delta (δ) - Guides/Elders/Hunters; And Omega (ω) - can follow all the wolves and solve them constantly.

Alpha, beta, and delta levels are considered the first, second, and third-best solutions. In correlation-based FS, if the deviation between two features is below a threshold, values obtained from records fall into any subset for deletion or selection. Therefore, more than these characteristics are needed to determine by its label. A value without deviation (i.e. 0) is called an auxiliary value. Thus, S should be optimized to improve feature selection further. The optimization process begins with initializing an initial population. A subset designated from PCRFE is considered the initial population of wolves, and n is the number of chosen features. Throughout the hunt, the wolf is enclosed by prey, meaning. Equations 35 to 38 show that the optimization benefits from detecting the diversity of features and improving the classification accuracy.

$$D = \left|E \times X_p - X_t\right| \quad (35)$$

$$\mathrm{X_{(t+1)}} = \left|\mathrm{X_{p(t)}} - \mathrm{A} \times \mathrm{D}\right| \quad (36)$$

$$\mathrm{E} = 2 \times \mathrm{rnd1} \quad (37)$$

$$A = |2a \times rnd2 - a| \quad (38)$$

Where, $\mathrm{X_p}$ –prey location, $\mathrm{X_t}$- grey wolf of the location, t- iteration, rnd1, rnd2 – random vectors in the range [0, 1], a ∈[0, 2] signified follows as equations 39.

$$a = 2 - t \times \frac{2}{Max.no\ of\ iterations} \quad (39)$$

Modifying the coefficient vectors E and A can change the optimal grey wolf position. The alpha (α), beta (β), and delta (δ) are answerable for prey assignments. The residual wolves modified their locations according to the best three solutions, as shown in equations 40 to 46.

$$\bar{X}_1 = X_\alpha - A_1 \times D_\alpha \quad (40)$$

$$\bar{X}_2 = X_\beta - A_2 \times D_\beta \quad (41)$$

$$\bar{X}_3 = X_\delta - A_3 \times D_\delta \quad (42)$$

$$\mathrm{X_{(t+1)}} = \frac{\bar{\mathrm{X}}_1+\bar{\mathrm{X}}_2+\bar{\mathrm{X}}_3}{3} \quad (43)$$

$$\mathrm{D_\alpha} = \left|\mathrm{E_1} \times \mathrm{X_\alpha} - \mathrm{X}\right| \quad (44)$$

$$\mathrm{D_\beta} = \left|\mathrm{E_2} \times \mathrm{X_\beta} - \mathrm{X}\right| \quad (45)$$

$$\mathrm{D_\delta} = \left|\mathrm{E_3} \times \mathrm{X_\delta} - \mathrm{X}\right| \quad (46)$$

|A|<1, the wolf updates its station between its present condition and the prey's position when it attacks the prey. Compared to the standard GWO, the position update is improved with the represented in Equation (47),

$$X_{(t+1)} = c_1 r_1 \left(\sum_{i=1}^{3} w_i * X_i(t)\right) + c_2 r_2 \left(\sum_{i=1}^{3} X_{ibest} * X_i(t)\right) \quad (47)$$

Where $\mathrm{c_1}$- social learning factor, $\mathrm{c_2}$- cognitive learning factor, $\mathrm{r_1}$,$\mathrm{r_2}$- random variables in the range [0,1]. X1, X2, and X3 are determined from Equations40, 41, and 42. $\mathrm{X_{ibest}}$- a grey wolf that has the best position. The set value $\mathrm{w_1}$, $\mathrm{w_2}$, and $\mathrm{w_3}$ – coefficient of inertia weight calculated as in Equations (48), (49),

and (50)

$$w_1 = \frac{|X_1|}{|X_1+X_2+X_3|} \quad (48)$$

$$w_2 = \frac{|X_2|}{|X_1+X_2+X_3|} \quad (49)$$

$$w_3 = \frac{|X_3|}{|X_1+X_2+X_3|} \quad (50)$$

Fig. 3: Optimal feature selection using PCRFE-GWO

The alpha, beta, and delta wolves leave their search space and unite when they raid the prey. The coefficient vector A takes random values in the range [-1, 1] to exclude the wolf from the target. All the optimized attributes are moved to a set called the Number of Selected Feature Sets (NFS). The selected and unselected features. The workflow of the proposed feature selection algorithm is shown in Figure 3.

Algorithm: (PCRFE-GWO)

Input: Normalized data set D, initial population X, maximum no of iteration tm, size of dataset N, number of features n, control parameter a, and learning factors c1 and c2

Output: Optimized feature subset

Step 1: For $i = 1\ to\ N$

Step 2: For $j = 1\ to\ n$

Step 3: Compute the correlation coefficient of the feature using the Equation (43)

Step 4: Eliminate the components using the PCRFE Equation (44)

Step 5: If ($PCRFE(x_i) \geq$ threshold, then

Step 6: Add the parts to the subset

Step 7: End if

Step 8: End for

Step 9: for t=1 to tm

Step 10: For $i = 1\ to\ N$

Step 11: For j = 1 to n

Step 12: CalculateD_α,D_β and $D_\delta$using Equations (44), (45) and (46)

Step 13: Calculate the coefficient of the weight w1, w2 and w3 using Equations (28), (29) and (30)

Step 14: Update the position of the grey wolf using Equations (41), (42), (23) and (47)

Step 15: End for

Step 16: End for

Step 17: End For

The classification unit uses DCNN as a deep learning technique to classify CVD datasets. CNN processes images as input with grayscale images with 2D representation and color images with 3D models. Also, the proposed TCNN with five layers can transform and estimate the features selected from the feature selection algorithm into an 11 × 11 array. Later, convolutional, pooling, input, hidden and output layers are fully integrated. Also, convolutional and pooling layers work with activation functions. DCNN can use a sigmoid activation function for binary classification and a softmax activation function for multiclass type to transform data from information to squared layers through hidden layers. The binary classification refers to the process of categorizing CVD data into two distinct classes: the presence of CVD (positive class - 1) and the absence of CVD (negative class-0). Also, a convolutional layer can use Equation 51 to complete the convolution process with multiple kernel values associated with biases and weights.

$$C_{x_i,y_i} = \sum_{i=1}^{p*q} w_i v_i \quad (51)$$

Where kernel k=p*q size, w_i −weight and v_i = image luminance value of the image dimension x_i, y_i After curling, the dimensions were reduced to 2×2 in a pooling step, a bias value, b, is added

between the input and hidden layers, and the activation function is h.

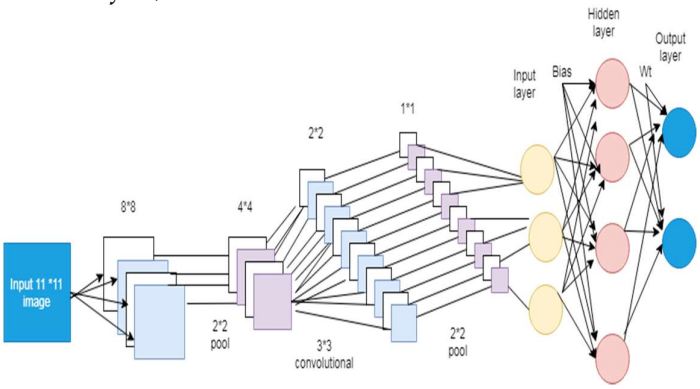

Fig. 4. Proposed CDNN architecture

To achieve this, the proposed Deep Convolutional Neural Network (DCNN) employs the sigmoid activation function. The proposed DCNN is illustrated in Figure 4 and takes an 11-by-11-dimensional array as input to the input layer.

Equations 52 and 53 utilize a smooth maximum activation function for multivariate classification and a sigmoid function as the activation function, producing a probability value between 0 and 1 in binary classification tasks with four hidden layers.

$$\text{sigmoid (h)} = \frac{1}{1+e^{-x_i}} \quad (52)$$

$$\text{softmax}(x_i) = \frac{e^{x_i}}{\sum_{j=1}^{n} e^{x_j}} \quad (53)$$

The hidden layer can process the input from the input layer and achieve activation processes to create the output based on the weight values. A hidden layer with a non-linear loss function can be described by Equation (54).

$$z_{x,y} = h \sum_{i=1}^{k} w_i v_i \quad (54)$$

The loss values for the actual and predicted values can be evaluated using Equation 55 as an activation function h. Furthermore, DL improves the results of neural networks based on minimizing the loss function.

$$\text{loss}(\text{input}_n, \text{output}_n) = \frac{1}{n}\sum_{i=1}^{n} d(\text{output}_i, f(\text{input}_i)) \quad (55)$$

From Figure 4, the input data set is normalized initially. The proposed feature selection algorithm chooses a subset of features based on the Pearson correlation method and removes features using recursive feature elimination. A subset of selected features is optimized using an evolutionary algorithm called GWO-DCNN to find the best features that increase the classification accuracy with enhanced location updates. A DL technique called DCNN is then used to classify the dataset with the best features. Due to the optimization technique and DL algorithms, the proposed algorithm can be efficient and promising.

Experiment and Result Analysis

This section discusses the efficiency of the proposed implementation using the CVD disease dataset collected from an online repository. It includes the simulation environment setup, performance evaluation, and comparison models for disease prediction.

4.1 Simulation environment setup

The simulation experiment is performed using Python 3.11.1 in a 64-bit Windows 10 OS with an Intel Core i5 processor (2.20 GHz) and 16GB RAM. The evaluation process is based on a confusion matrix that helps determine the accuracy of the proposed method. The GWO-DCNN model selects features based on maximum support weight values, validating training features with high precision. The performance of the GWO-DCNN model is measured using various evaluation metrics, including accuracy, precision, recall, and F1-score.

The accuracy is determined using the following formula:

$$Accuracy = \frac{TN+TP}{(TP+FP+FN+TN)} \quad (56)$$

The results obtained are based on the analysis of biomedical history, particularly lymphoma marrow samples.

Table 2. Simulation Parameters for PD Prediction

Parameters	Values
Tool	Anaconda
Language	Python
Name of the dataset	Cardio-CVD-HCD dataset
No of records	5000

Table 2 outlines the essential settings for the simulation, including the programming language, dataset specifications, and tools used. The dataset comprises 5000 records, ensuring a comprehensive evaluation of the model's predictive capabilities.

4.2 PD Dataset Description

The CVD disease datasets were collected from the Kaggle repository (available at https://www.kaggle.com/datasets/debasisdotcom/CVD-disease-detection). The dataset consists of 24 features and 500 records, representing patients with PD symptoms. The dataset distribution, providing insight into the different attributes analyzed. A visual representation of feature distributions helps in understanding data trends and feature importance.

4.3 Performance evaluation metrics

The effectiveness of the proposed model is determined by its ability to distinguish healthy individuals from PD patients. The performance is assessed using four key evaluation metrics:

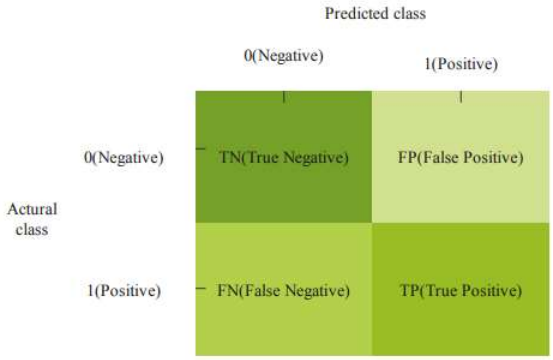

Fig. 5. Confusion Matrix

The confusion matrix presented in Figure 5 illustrates the true positives (TP), true negatives (TN), false positives (FP), and false negatives (FN) identified during prediction. It provides a detailed breakdown of how well the model classifies PD patients and non-PD individuals, highlighting misclassifications and successful detections.

The following metrics are calculated based on these values:

a) Precision measures the proportion of correctly identified positive cases:

$$\text{Precision} = \frac{\sum \text{True}_{\text{positive}}}{\sum \text{True}_{\text{positive}} + \text{False}_{\text{positive}}} * 100 \quad (57)$$

b) Recall assesses the proportion of actual positives correctly identified:

$$Recall = \frac{\sum True_{positive}}{\sum True_{positive} + False_{negative}} * 100 \quad (58)$$

c) F1-score provides a balance between precision and recall:

$$\text{F1-score} = \sum 2X \frac{Pre * Rec}{Pre + Rec} * 100 \quad (59)$$

d) Accuracy measures overall correctness:

$$\text{Accuracy} = \frac{\sum \text{True}_{\text{positive}} + \text{True}_{\text{negative}}}{\sum \text{True}_{\text{positive}} + \text{False}_{\text{negative}} + \text{False}_{\text{positive}} + \text{True}_{\text{negative}}} * 100 \quad (60)$$

4.4 Comparison model for PD prediction

The proposed FGWO-CNN model is compared against existing algorithms such as Recursion Enhanced Random Forest with an Improved Linear Model (RERF-ILM) and QMBC.

4.4.1 Precision Performance Comparison

Table 3. Precision Performance Comparison

Precision performance in %			
Comparison methods/ No of records	**RERF-ILM**	**QMBC**	**FGWO-CNN**
1000	54.3	65.2	72.3
2000	60.5	69.8	75.1
3000	69.9	83.2	86.5
4000	72.5	88.7	95.9

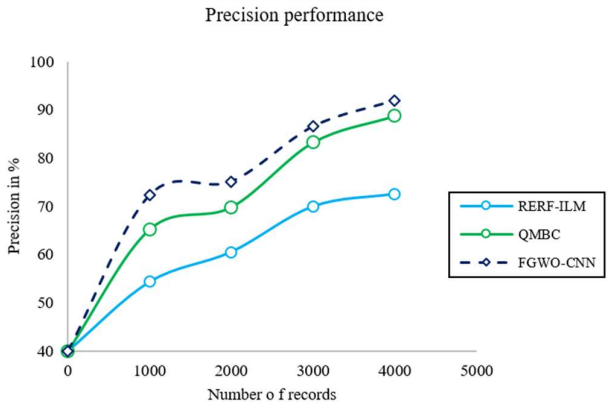

Fig. 6: Precision performance

Table 3 compares the precision of different classification models over increasing dataset sizes. The FGWO-CNN model consistently outperforms the baseline models, demonstrating higher precision values, which indicate a lower false-positive rate. Figure 6 highlights the improvement in precision across different methods. When evaluating the performance of the FGWO-CNN method in comparison to existing techniques, namely RERF-ILM and QMBC, the error rates observed indicate a substantial degree of variation. Specifically, the precision associated with the FGWO-CNN approach is 72.5% compared to the RERF-ILM technique. Furthermore, a comparative analysis against QMBC reveals a precision of 88.7% for the FGWO-CNN method. The proposed FGWO-CNN model outperforms existing techniques, achieving 95.9% precision for 4000 records, validating its reliability in disease prediction.

4.4.2. Recall Performance Comparison

Table 4. Recall Performance Comparison

Recall performance in %			
Comparison methods/ No of records	**RERF-ILM**	**QMBC**	**FGWO-CNN**
1000	53.2	68.3	72.8
2000	59.5	71.4	77.5
3000	67.8	83.7	86.2
4000	69.4	87.1	94.9

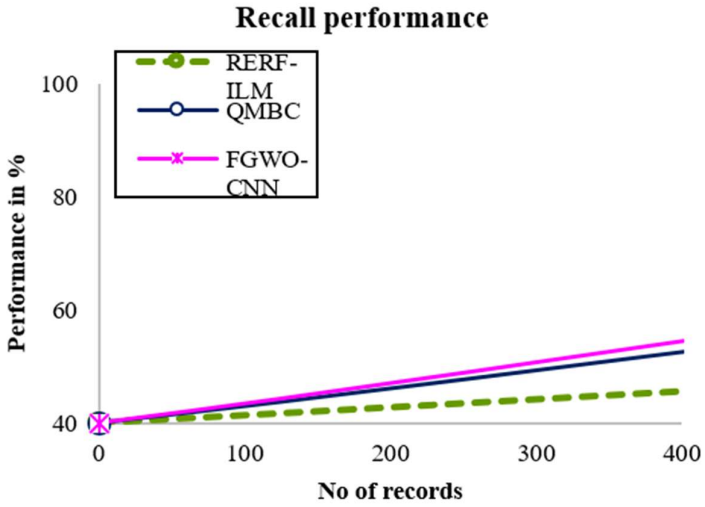

Fig. 7. Recall performance

Table 4 outlines the recall scores for different models, demonstrating the FGWO-CNN model's superior ability to correctly identify positive cases while minimizing false negatives. In assessing the FGWO-CNN method's performance relative to existing techniques such as RERF-ILM and QMBC, the observed recall shows significant variation. The FGWO-CNN approach achieves a recall rate of 69.7% when compared to RERF-ILM. Additionally, an analysis against QMBC shows that the FGWO-CNN method has a precision of 87.1%. As illustrated in Figure 7, the FGWO-CNN model demonstrates the highest recall performance, attaining 94.9% with 4000 records. This confirms its ability to correctly identify PD patients with fewer false negatives compared to RERF-ILM and QMBC.

4.4.3. F1-Score Performance

Table 5. F1-Score Performance

F1-score performance in %			
Comparison methods/ No of records	**RERF-ILM**	**QMBC**	**FGWO-CNN**
1000	59.4	66.3	72.8
2000	65.8	76.5	78.5
3000	70.1	87.9	90.6
4000	74.3	89.4	95.3

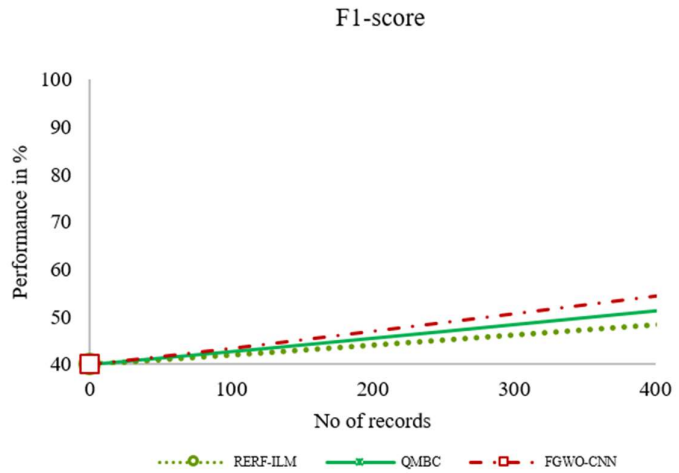

Fig. 8. F1-score performance

Table 5 and Figure 8 compare the F1-score across different classification models. The F1-score shows significant variation in assessing the FGWO-CNN method's performance relative to existing techniques such as RERF-ILM and QMBC. The FGWO-CNN approach achieves an F1-score of 74.3% when compared to RERF-ILM. Additionally, an analysis against QMBC shows that the FGWO-CNN method has a precision of 89.4%. The FGWO-CNN model achieves the highest F1-score (95.3%) for 4000 records, indicating superior classification performance, ensuring that the FGWO-CNN model is effective in reducing misclassification error.

4.4.4. Classification Performance Analysis

Table 6. Classification Performance Analysis

Classification performance in %			
Comparison methods/ No of records	**RERF-ILM**	**QMBC**	**FGWO-CNN**
1000	58.5	66.8	73.3
2000	63.4	70.9	76.5
3000	70.3	85.8	87.2
4000	73.6	89.9	95.8

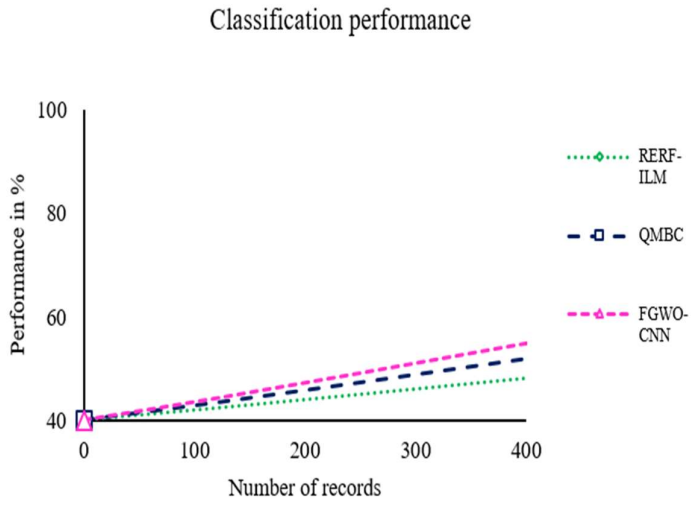

Fig. 9. Classification performance

Table 6 presents the classification performance of different models across various dataset sizes. The FGWO-CNN model consistently outperforms RERF-ILM and QMBC, achieving the highest classification performance as the number of records increases. Figure 9 illustrates the classification performance of the FGWO-CNN method for predicting PD across different dataset sizes. The results demonstrate that as the number of records increases, the classification performance also improves. The FGWO-CNN model attains a classification accuracy of 94.5% for 4000 records, indicating its robustness in predicting PD with high precision. The increasing trend in performance suggests that the proposed model effectively generalizes across larger datasets, making it a reliable choice for real-world applications in PD detection. The classification performance varies considerably when evaluating the FGWO-CNN method against existing techniques like RERF-ILM and QMBC. When compared to RERF-ILM, the FGWO-CNN approach achieves a classification accuracy of 73.6%. Furthermore, an assessment against QMBC reveals that the FGWO-CNN method boasts a precision rate of 89.9%.

4.4.5. False Classification Performance Analysis

Table 7. False Classification Performance Analysis

False Classification performance (%)			
Comparison Methods / Number of records	**1000**	**3000**	**4000**
RERF-ILM	32.1	25.1	18.3
QMBC	28.9	22.6	16.2
FGWO-CNN	13.8	12.4	10.6

Table 7 evaluates the false classification rates of different models. The FGWO-CNN model achieves the lowest false classification rate, demonstrating improved accuracy in classification.

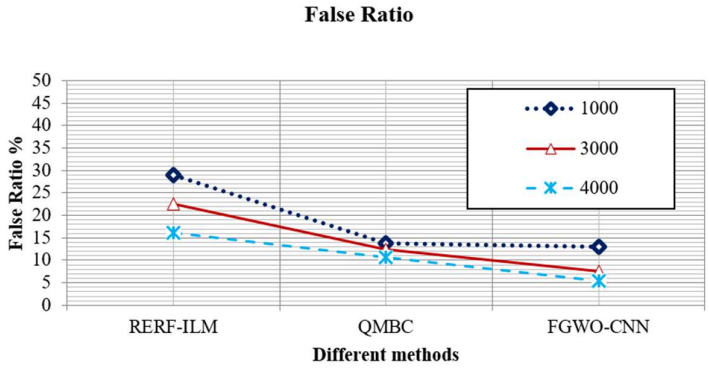

Fig. 10. False Classification Ratio Analysis

Figure 10 depicts the false classification ratio comparison. The FGWO-CNN model processes data effectively by eliminating noise and improving classification accuracy, resulting in significantly lower false classification rates. When evaluating the performance of the FGWO-CNN method in comparison to existing techniques, namely RERF-ILM and QMBC, the error rates observed indicate a substantial degree of variation. Specifically, the false rate associated with the FGWO-CNN approach is 18.3% compared to the RERF-ILM technique. Furthermore, a comparative analysis against QMBC reveals an error rate of 16.2% for the FGWO-CNN method. Finally, an error rate of 10.6% emerges when considering the disparities between the proposed FGWO-CNN and the performance of the previous techniques.

4.4.6. CVD disease prediction accuracy

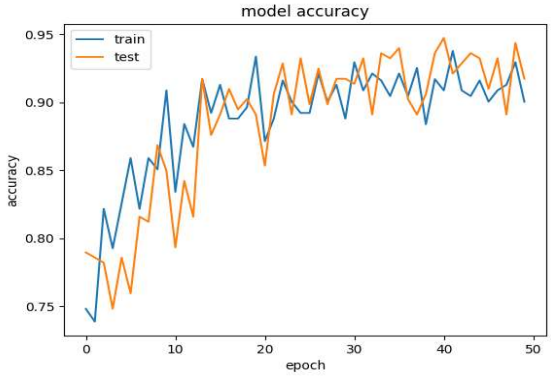

Fig. 11. CVD disease prediction accuracy

Figure 11 highlights the accuracy performance of the proposed method in predicting CVD risk

levels during both training and validation phases. The FGWO-CNN model efficiently categorizes patients based on their risk level by leveraging optimized feature selection and classification techniques. The dataset undergoes rigorous preprocessing, ensuring that only relevant clinical attributes contribute to the classification process. The classification threshold margin is used to refine the model's decision boundary, leading to a notable improvement in predictive accuracy. The results confirm that the proposed FGWO-CNN model delivers high classification accuracy, making it a reliable solution for CVD risk prediction and patient monitoring

Conclusion

The intelligent big data analytics model for efficient CVD Prediction integrates ANFIS and GWO-CNN techniques to enhance both the accuracy and efficiency of disease prediction. By implementing an advanced feature scaling model based on Heart Rate Variability (HRV), the system effectively reduces dimensionality while identifying critical disease patterns, particularly in elderly patients. In this framework, the Adaptive Neuro-Fuzzy Inference System (ANFIS) plays a crucial role in feature selection, utilizing membership functions and fuzzy rule sets to focus on the most relevant attributes, thereby improving predictive performance. The quantitative evaluation of the proposed model demonstrates near-optimal results, achieving over 96% precision, recall, and F-score, while maintaining a low error rate and reduced time complexity. These results indicate the model's robustness and reliability for practical applications in healthcare. For future advancements, increasing the number of features will not be constrained by static, unmodifiable attributes, as further refinements in dimensionality reduction such as bias weight adjustments—can enhance the model's adaptability. This approach enables dynamic feature selection, improving the model's ability to process diverse input data across various medical conditions. Additionally, the spectral margin feature evaluation, an advanced deep learning technique, can be further fine-tuned to optimize classification accuracy. This study provides a strong foundation for the application of big data analytics and deep learning in the early identification and management of CVDs. The model holds significant potential for real-world implementation, offering personalized recommendations and predictive insights for individuals at high risk of CVDs. By integrating developmental learning, this approach could further enhance healthcare systems, supporting both individualized patient care and population-level risk assessment for improved medical decision-making.

Conflicts of Interest

The author(s) declare(s) that there is no conflict of interest regarding the publication of this paper..

References

Zhou, C., Dai, P., Hou, A. et al. A comprehensive review of deep learning-based models for heart disease prediction. Artif Intell Rev 57, 263 (2024). https://doi.org/10.1007/s10462-024-10899-9.

Naser, M. A., Majeed, A. A., Alsabah, M., Raad, T., & Kaky, K. M. (2024). A Review of Machine Learning's Role in Cardiovascular Disease Prediction: Recent Advances and Future Challenges. Algorithms, 17(2), 78. https://doi.org/10.3390/a17020078.

A. M. Qadriet al., "Effective feature engineering technique for heart disease prediction with machine learning" in IEEE Access, vol. 11, pp. 56214-56224, 2023, doi:10.1109/ACCESS.2023.3281484.

A. A. Almazroiet al., "A clinical decision support system for heart disease prediction using deep learning" in IEEE Access, vol. 11, pp. 61646-61659, 2023, doi:10.1109/ACCESS.2023.3285247.

Ram Kumar, R. P., et al. "Investigations on cardiovascular diseases and predicting using machine learning algorithms." Cogent Engineering 11.1 (2024): 238638.

X. Yuan et al., "A stable AI-based binary and multiple class heart disease prediction model for IoMT" in IEEE Trans. Ind. Inform., vol. 18, no. 3, pp. 2032-2040, Mar.2022, doi:10.1109/TII.2021.3098306.

Baghdadi, N. A., Farghaly Abdelaliem, S. M., Malki, A., Gad, I., Ewis, A., & Atlam, E. (2023). Advanced machine learning techniques for cardiovascular disease early detection and diagnosis. Journal of Big Data, 10(1), 1-29. https://doi.org/10.1186/s40537-023-00817-1.

G. N. Ahmadet al., "Efficient medical diagnosis of human heart diseases using machine learning techniques with and without Grid Search CV" in IEEE Access, vol. 10, pp. 80151-80173, 2022, doi:10.1109/ACCESS.2022.3165792.

Manikandan, G., Pragadeesh, B., Manojkumar, V., Karthikeyan, A., Manikandan, R., & Gandomi, A. H. (2023). Classification models combined with Boruta feature selection for heart disease prediction. Informatics in Medicine Unlocked, 44, 101442. https://doi.org/10.1016/j.imu.2023.101442.

G. N. Ahmadet al., "Comparative study of optimum medical diagnosis of human heart disease using machine learning technique with and without sequential feature selection" in IEEE Access, vol. 10, pp. 23808-23828, 2022, doi:10.1109/ACCESS.2022.3153047.

Gayathri, R., et al. "Enhancing heart disease prediction with reinforcement learning and data augmentation." Systems and Soft Computing 6 (2024): 200129.

Joshi, Neeraja, and Tejal Dave. "Improved accuracy for heart disease diagnosis using machine learning techniques." Journal of Informatics and Web Engineering 4.1 (2025): 42-52.

S. E. A. Ashriet al., "HDPF: Heart disease prediction frame work based on hybrid classifiers and genetic algorithm" in IEEE Access, vol. 9, pp. 146797-146809, 2021, doi:10.1109/ACCESS.2021.3122789.

A. Rahimet al., "An integrated machine learning framework for effective prediction of cardio vascular diseases" in IEEE Access, vol. 9, pp. 106575-106588, 2021, doi:10.1109/ACCESS.2021.3098688.

D. Cenittaet al., "ischemic heart disease prediction using optimized squirrel search feature selection algorithm" in IEEE Access, vol. 10, pp. 122995-123006, 2022, doi:10.1109/ACCESS.2022.3223429.

Saikumar, K., and V. Rajesh. "A machine intelligence technique for predicting cardiovascular disease (CVD) using Radiology Dataset." International Journal of System Assurance Engineering and Management 15.1 (2024): 135-151.

Ogunpola, Adedayo, et al. "Machine learning-based predictive models for detection of cardiovascular diseases." Diagnostics 14.2 (2024): 144.

Ramesh, B., and Kuruva Lakshmanna. "A novel early detection and prevention of coronary heart disease framework using hybrid deep learning model and neural fuzzy inference system." IEEE Access 12 (2024): 26683-26695.

Trigka, Maria, and Elias Dritsas. "Improving Cardiovascular Disease Prediction With Deep Learning and Correlation-Aware SMOTE." IEEE Access (2025).

Khan, Hira, et al. "Heart disease prediction using novel ensemble and blending based cardiovascular disease detection networks: EnsCVDD-Net and BlCVDD-Net." IEEE Access (2024).

R. Kapilaet al., "Heart disease prediction using novel Quine McCluskey binary classifier (QMBC)" in IEEE Access, vol. 11, pp. 64324-64347, 2023, doi:10.1109/ACCESS.2023.3289584.

A. Abdellatifet al., "An effective heart disease detection and severity level classification model using machine learning and hyper parameter optimization methods" in IEEE Access, vol. 10, pp. 79974-79985, 2022, doi:10.1109/ACCESS.2022.3191669.

Ahmed, Mohammed, and Idress Husien. "Heart disease prediction using hybrid machine learning: A brief review." Journal of Robotics and Control (JRC) 5.3 (2024): 884-892.

H. Siddiquiet al., "A survey on machine and deep learning models for childhood and adolescent obesity" in IEEE Access, vol. 9, pp. 157337-157360, 2021, doi:10.1109/ACCESS.2021.3131128.

Ullah, Tahseen, et al. "Machine learning-based cardiovascular disease detection using optimal feature selection," IEEE Access 12 (2024): 16431-16446.

A. Ishaqet al., "Improving the prediction of heart failure patients' survival using SMOTE and effective data mining techniques" in IEEE Access, vol. 9, pp. 39707-39716, 2021, doi:10.1109/ACCESS.2021.3064084.

Venkatesh, C., et al. "An automatic diagnostic model for the detection and classification of cardiovascular diseases based on swarm intelligence technique." Heliyon 10.3 (2024).

Naeem, Awad Bin, et al. "Heart disease detection using feature extraction and artificial neural networks: A sensor-based approach." IEEE Access (2024).

B. Xiaoet al., "Follow the sound of children's heart: A deep-learning-based computer-aided pediatric CHD diagnosis system" in IEEE Internet Things J., vol. 7, no. 3, pp. 1994-2004, Mar.2020, doi:10.1109/JIOT.2019.2961132.

Rehman, Moiz Ur, et al. "Predicting coronary heart disease with advanced machine learning classifiers for improved cardiovascular risk assessment." Scientific Reports 15.1 (2025): 13361.

Liao, Y., Tang, Z., Gao, K., &Trik, M. (2024). Optimization of resources in intelligent electronic health systems based on Internet of Things to predict heart diseases via artificial neural network. Heliyon, 10(11).

Molamasoumi, A., Sadeghizadeh, H., Rajabi, M., Hajam, M. A., &Khanday, A. M. U. D. (2023). Neuro Fuzzy GreyWolf Optimisation Method for Diagnosing the Liver Disorders. Preprints, 2023091704...